Performance Analysis for BPSK Alamouti's Scheme with Distributed Transmit Antennas

LI Zhi-gang and TANG You-xi

(National Key Laboratory of Science and Technology on Communications, University of Electronic Science and Technology of China　Chengdu　611731)

Abstract　An approximate expression of bit error rate (BER) is derived for a circular cell distributed antenna system with space-time block coding based on Alamouti's scheme and utilizing binary phase shift keying (BPSK) modulation. The analysis is carried out on considering the effects of path loss, log-normal shadowing, multipath fading and background noise. A simulation is carried out under the condition of two transmit and one received antennas, single-path Rayleigh fading channels, antenna spacing of 200 m, and standard deviation of shadowing of 8 dB. The simulation results show that, the numerical results match the simulation results well, and at the BER of 3×10^{-1}, the proposed method is superior by about 1.4 dB to the traditional methods in bit signal-to-noise ratio.

Key words　bit error rate;　distributed antenna systems;　large-scale fading;　space-time block coding

分布式发射天线下BPSK Alamouti方案性能分析

李志刚，唐友喜

(电子科技大学通信抗干扰技术国家级重点实验室　成都　611731)

【摘要】在分布式发射天线系统中，针对圆形小区下基于Alamouti空时分组编码和采用BPSK调制的情况，推导了误比特性能的近似解析表达式。理论推导过程考虑了路径损耗、阴影衰落、单径瑞利衰落和背景噪声的影响。在2发1收、单径瑞利衰落信道、200 m发射天线间距以及8 dB阴影标准差的条件下进行仿真，结果表明，所提方法的数值分析结果和计算机仿真结果是相吻合的，且在比特误码率为3×10^{-1}时，与传统方法相比，该文方法在性能上有约1.4 dB的比特信噪比增益。

关　键　词　比特误码率;　分布式天线系统;　大尺度衰落;　空时分组码

Apart from the in-depth research on co-located antenna systems (CAS), distributed antenna systems (DAS) have been attracting worldwide interest and are expected to be one of the promising techniques in the next generation wireless communication systems[1-3]. Space-time block coding (STBC), which was first proposed by Alamouti[4] for systems with two transmit antennas, is a superb candidate for next-generation wireless systems.

However, there is little information on the analysis of exact or approximate expressions of bit error rate (BER) for space-time block coding with distributed transmit antennas.

In Ref. [5], a tight closed-form upper bound was presented for the BER of space-time block coding in Rician and log-normal fading channel, respectively. An expression of BER over small-scale fading and large-scale fading was given in Ref. [2], but it was an approximate expression in high signal-to-noise ratio (SNR) region.

This letter derives an approximate BER for arbitrary SNR for DAS with space-time block coded based on Alamouti's scheme and utilizes binary phase shift keying (BPSK) modulation over composite exponential/log-normal fading.

1 System Model

1.1 Transmitter

For DAS, two transmit antennas connected to a single base station by fiber optic or coaxial cables are located at different places of a cell. For practical reason, the mobile station (MS) is assumed to have a single antenna. The separation distance between the antennas is denoted by D ($\gg \lambda$, where λ is the wavelength). The separation distance between the MS and the kth transmit antenna (TX$_k$) is denoted by d_k (k=1,2). We assume a system with ideal synchronization. We also assume a noise-limited environment. This assumption holds for an isolated cell or a multicell system with large frequency reuse distance where the interference is small compared with the thermal noise[6].

1.2 Receiver

The output of the STBC decoder can be given by Ref. [4]:

$$R = \sqrt{P'/2}\,\|h\|\,X + W \qquad (1)$$

where P' is the total transmitted power at the base station, h is a channel vector of size 2×1, $\|h\|$ is Euclidean norm of h, X represents the transmitted symbol, and W is additive complex Gaussian noise with zero mean and variance N_0. The coefficient $\sqrt{P'/2}$ ensures that the total transmitted power is P'.

In DAS, the transmit antennas are spaced by large distance. Hence, the channel model involves not only small-scale fading but also large-scale fading. Therefore, the channel vector can be expressed as:

$$h = [h_1\sqrt{S_1}, h_2\sqrt{S_2}]^T \qquad (2)$$

where h_k represents composite multipath/shadowing fading, and S_k is a factor that captures the effects of path loss for the TX$_k$-MS link (k=1,2).

We model h_k as a complex composite exponential/ log-normal random variable. The composite exponential/log-normal probability density function (PDF) of SNR γ_k can be presented as[7]:

$$P_{\gamma_k}(\gamma_k) = \int_0^\infty \frac{1}{\Omega_k}\exp\left(-\frac{\gamma_k}{\Omega_k}\right)\frac{\xi}{\sqrt{2\pi}\sigma_k\Omega_k} \times$$
$$\exp\left[-\frac{(10\lg\Omega_k - \mu_k)^2}{2\sigma_k^2}\right]d\Omega_k \qquad (3)$$

where Ω_k is the average received power,

$\xi = 10/\ln 10$, μ_k(dB) = $10\lg\bar{\gamma}_k$ and σ_k(dB) are the mean and standard deviation of $10\lg\Omega_k$, respectively, and $\bar{\gamma}_k$ is the average SNR per bit.

We model S_k as follows[8]:

$$S_k = \begin{cases} \left(\dfrac{\lambda}{4\pi}\right)^2 d_k^{-2} & d_k \leqslant \Upsilon \\ (h_b h_s)^2 d_k^{-4} & d_k > \Upsilon \end{cases} \qquad (4)$$

where λ is the wavelength, h_b is the transmit antenna height, h_s is the MS antenna height, and $\Upsilon = 4\pi h_b h_s / \lambda$ denotes the break point.

2 BER Analysis

According to the described channel model, the instantaneous power received from TX$_k$ can be expressed as:

$$P_k^r = \frac{1}{2}P'|h_k|^2 S_k \qquad (5)$$

Then, the total received power is $P^r = \sum_{k=1}^{2} P_k^r$. Under the assumption of BPSK modulation, the BER, conditioned on the mean SNR $\bar{\gamma}_1 = P'S_1/2N_0$ and $\bar{\gamma}_2 = P'S_2/2N_0$, can be expressed as:

$$P_e(\bar{\gamma}_1,\bar{\gamma}_2) = \int_0^\infty\int_0^\infty Q(\sqrt{2\gamma})f(\gamma_1,\gamma_2\,|\,\bar{\gamma}_1,\bar{\gamma}_2)d\gamma_1 d\gamma_2 \qquad (6)$$

where $Q(\cdot)$ is the Gaussian probability function[9], $\gamma = \sum_{k=1}^{2}\gamma_k$ is the total instantaneously received SNR, $\gamma_k = P_k^r/N_0$ represents the instantaneous SNR received from TX$_k$, and $f(\gamma_1,\gamma_2\,|\,\bar{\gamma}_1,\bar{\gamma}_2)$ is the joint conditional PDF of γ_1 and γ_2. According to the given channel model, γ_1 and γ_2, conditioned on $\bar{\gamma}_1$ and $\bar{\gamma}_2$, are independent and identically distributed composite exponential/log-normal random variables. Hence,

$$f(\gamma_1,\gamma_2\,|\,\bar{\gamma}_1,\bar{\gamma}_2) = P_{\gamma_1}(\gamma_1\,|\,\bar{\gamma}_1)P_{\gamma_2}(\gamma_2\,|\,\bar{\gamma}_2) \qquad (7)$$

where $P_{\gamma_k}(\gamma_k\,|\,\bar{\gamma}_k)$ is the conditional PDF of γ_k in Eq. (3). Using Craig's formula for the Gaussian Q-function[9], $Q(\sqrt{2\gamma})$ can be expressed as:

$$Q(\sqrt{2\gamma}) = \frac{1}{\pi}\int_0^{\pi/2}\exp\left(-\frac{\gamma}{\sin^2\theta}\right)d\theta =$$
$$\frac{1}{\pi}\int_0^{\pi/2}\prod_{k=1}^{2}\exp\left(-\frac{\gamma_k}{\sin^2\theta}\right)d\theta \qquad (8)$$

where θ is an integral parameter. Then, it follows from Eq. (6) that:

$$P_e(\bar{\gamma}_1,\bar{\gamma}_2) = \int_0^\infty \int_0^\infty \left[\frac{1}{\pi}\int_0^{\pi/2}\prod_{k=1}^2 \exp\left(-\frac{\gamma_k}{\sin^2\theta}\right)d\theta\times\right.$$

$$\left.\prod_{k=1}^2 P_{\gamma_k}(\gamma_k|\bar{\gamma}_k)\,d\gamma_1 d\gamma_2\right] \tag{9}$$

After exchanging the integral order of θ and γ_k in Eq. (9), we have:

$$P_e(\bar{\gamma}_1,\bar{\gamma}_2) = \frac{1}{\pi}\int_0^{\pi/2}\left\{\prod_{k=1}^2\int_0^\infty\left[\exp\left(-\frac{\gamma_k}{\sin^2\theta}\right)\times\right.\right.$$

$$\left.\left. P_{\gamma_k}(\gamma_k|\bar{\gamma}_k)\right]d\gamma_k\right\}d\theta \tag{10}$$

Based on the moment generating function (MGF) of composite exponential/log-normal PDF[7], we have:

$$\int_0^\infty\left[\exp\left(-\frac{\gamma_k}{\sin^2\theta}\right)P_{\gamma_k}(\gamma_k|\bar{\gamma}_k)\right]d\gamma_k =$$

$$\frac{1}{\sqrt{\pi}}\int_{-\infty}^\infty\left(1+\frac{1}{\sin^2\theta}10^{(x\sqrt{2}\sigma_k+\mu_k)/10}\right)^{-1}e^{-x^2}dx \tag{11}$$

It can be easily derived that:

$$10^{(x\sqrt{2}\sigma_k+\mu_k)/10} = \bar{\gamma}_k\times10^{x\sqrt{2}\sigma_k/10} \tag{12}$$

Substituting Eq. (11) and Eq. (12) into Eq. (10) yields:

$$P_e(\bar{\gamma}_1,\bar{\gamma}_2) = \frac{1}{\pi}\int_0^{\pi/2}\left\{\prod_{k=1}^2\left[\frac{1}{\sqrt{\pi}}\int_{-\infty}^\infty(1+\right.\right.$$

$$\left.\left.\frac{\bar{\gamma}_k}{\sin^2\theta}10^{x\sqrt{2}\sigma_k/10}\right)^{-1}e^{-x^2}dx\right]\right\}d\theta \tag{13}$$

The inner integral can be computed efficiently using a Gauss-Hermite quadrature integration[7,10], that is:

$$\frac{1}{\sqrt{\pi}}\int_{-\infty}^\infty\left(1+\frac{\bar{\gamma}_k}{\sin^2\theta}10^{x\sqrt{2}\sigma_k/10}\right)^{-1}e^{-x^2}dx =$$

$$\frac{1}{\sqrt{\pi}}\sum_{i=1}^n w_i\frac{\sin^2\theta}{\sin^2\theta+\bar{\gamma}_k\times10^{x_i\sqrt{2}\sigma_k/10}} \tag{14}$$

where $x_i(i=1,2,\cdots,n)$ are the zeros of the n-order Hermite polynomial $He_n(x)$ and $w_i(i=1,2,\cdots,n)$ are weight factors tabulated in Table 25.10 of Ref. [10] for values of n from 2 to 20. To get numerical results in section IV, of Ref. [10] we can choose $n=20$ to compute BER as the approximate results. Then, we have:

$$P_e(\bar{\gamma}_1,\bar{\gamma}_2) = \frac{1}{\pi^2}\int_0^{\pi/2}\sum_{i=1}^n w_i\frac{\sin^2\theta}{\sin^2\theta+\bar{\gamma}_1 10^{x_i\sqrt{2}\sigma_1/10}}\times$$

$$\sum_{i=1}^n w_i\frac{\sin^2\theta}{\sin^2\theta+\bar{\gamma}_2 10^{x_i\sqrt{2}\sigma_1/10}}d\theta \tag{15}$$

If $\bar{\gamma}_1\neq\bar{\gamma}_2$, we spread the product of two polynomials in Eq. (15) as follows:

$$\left(\sum_{i=1}^n w_i a_i\right)\left(\sum_{i=1}^n w_i b_i\right) =$$

$$\sum_{i=1}^n w_i^2 a_i b_i + \sum_{1\leqslant i<j\leqslant n} w_i w_j(a_i b_j + a_j b_i) \tag{16}$$

Since

$$\frac{\sin^2\theta}{\sin^2\theta+c_1}\frac{\sin^2\theta}{\sin^2\theta+c_2} = 1 - \frac{c_1}{\sin^2\theta+c_1} -$$

$$\frac{c_2}{\sin^2\theta+c_2} + \frac{c_1 c_2}{c_2-c_1}\left(\frac{1}{\sin^2\theta+c_1}-\frac{1}{\sin^2\theta+c_2}\right) \tag{17}$$

and

$$\frac{1}{\pi}\int_0^{\pi/2}\frac{c}{\sin^2\theta+c}d\theta = \frac{1}{2}\sqrt{\frac{c}{1+c}} \tag{18}$$

we have:

$$\frac{1}{\pi}\int_0^{\pi/2}\frac{\sin^2\theta}{\sin^2\theta+c_1}\frac{\sin^2\theta}{\sin^2\theta+c_2}d\theta =$$

$$\frac{1}{2}\frac{c_2\psi(c_2)-c_1\psi(c_1)}{c_2-c_1} \tag{19}$$

where $c_1\neq c_2$, and ψ is a function of c, i.e. $\psi(c)=1-\sqrt{\dfrac{c}{1+c}}$. Letting $c_k^{(i)}=\bar{\gamma}_k 10^{x_i\sqrt{2}\sigma_1/10}$ $(k=1,2,\cdots,n)$ and using Eq. (19), $P_e(\bar{\gamma}_1,\bar{\gamma}_2)$ can be expressed as:

$$P_e(\bar{\gamma}_1,\bar{\gamma}_2) = \frac{1}{2\pi}\left\{\sum_{i=1}^n w_i^2\frac{c_2^{(i)}\psi(c_2^{(i)})-c_1^{(i)}\psi(c_1^{(i)})}{c_2^{(i)}-c_1^{(i)}}+\right.$$

$$\sum_{1\leqslant i<j\leqslant n}w_i w_j\left[\frac{c_2^{(j)}\psi(c_2^{(j)})-c_1^{(i)}\psi(c_1^{(i)})}{c_2^{(j)}-c_1^{(i)}}+\right.$$

$$\left.\left.\frac{c_2^{(i)}\psi(c_2^{(i)})-c_1^{(j)}\psi(c_1^{(j)})}{c_2^{(i)}-c_1^{(j)}}\right]\right\} \tag{20}$$

If $\bar{\gamma}_1=\bar{\gamma}_2$, we spread the product of two polynomials in Eq. (15) as follows:

$$\left(\sum_{i=1}^n w_i a_i\right)^2 = \sum_{i=1}^n w_i^2 a_i^2 + \sum_{i\neq j} w_i w_j a_i a_j \tag{21}$$

According to Ref. [7], we have:

$$\varphi(c)\triangleq\frac{1}{\pi}\int_0^{\pi/2}\left(\frac{\sin^2\theta}{\sin^2\theta+c}\right)^2 d\theta =$$

$$\frac{1}{2}\psi(c)\left[1-\frac{1}{2}(\psi(c)-1)(\psi(c)-2)\right] \tag{22}$$

Hence, $P_e(\bar{\gamma}_1,\bar{\gamma}_2)$ can be expressed as:

$$P_e(\bar{\gamma}_1,\bar{\gamma}_2) = \frac{1}{2\pi}\left\{\sum_{i=1}^n w_i^2\varphi(c_1^i)+\right.$$

$$\left.\sum_{i\neq j}w_i w_j\frac{c_1^{(j)}\psi(c_1^{(j)})-c_1^{(i)}\psi(c_1^{(i)})}{c_1^{(j)}-c_1^{(i)}}\right\} \tag{23}$$

3 Numerical and Simulation Results

Numerical results are provided to demonstrate the analysis developed in this letter and to compare it with simulation results. The approximate results are also compared with the ones obtained by Ref. [2]. The basic simulation parameters are tabulated in Table 1 as follows.

Table 1 Simulation parameters

parameter vitem	value
Total transmit power P' /mW	50
Transmit antenna height h_b /m	5
MS antenna height h_r /m	1.5
Wavelength λ /m	0.3
Radius of Cell R/m	250
Antenna Spacing D/m	200
Channel Bandwidth B/MHz	20

The total SNR is $\gamma = \sum_{l=1}^{2}\gamma_k = \sum_{l=1}^{2}P_k^r/N_0$ and noise power of receiver N_0 [8] is -174 dBm$+10\lg B$.
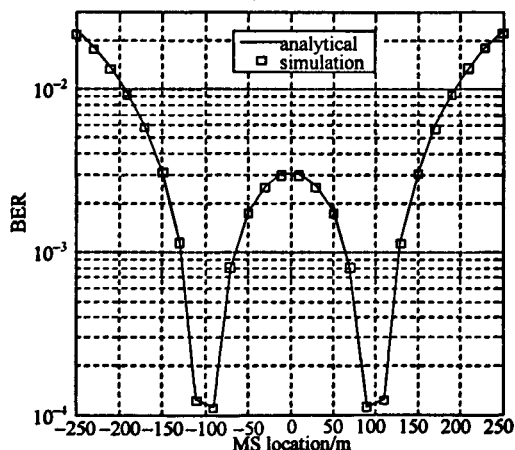

Fig. 1 BER performance of distributed Alamouti STBC versus MS location with $\sigma_k = 8$ dB along a line through the center of circular cell and TX$_k$

Fig. 1 shows the BER performance of distributed Alamouti STBC versus MS location with $\sigma_k = 8$ dB along a line through the center of circular cell and TX$_k$, where the transmit power of each transmit antenna is 25 mW. Curves are obtained both by analysis and simulation. From Fig. 1 we can observe that, theoretical analysis and simulation results match well for MS along the line. Furthermore, it can be obtained that the closer the distance between MS and transmit

antenna, the better the BER performance.

Fig. 2 shows the BER performance of distributed Alamouti STBC versus the SNR at $d_1 = 100$ m and $d_2 = 110$ m, with $\sigma_k = 4$ dB and 8 dB, respectively. Curves are obtained both by analysis and simulation. It can be seen that analysis results agree well with theoretical ones. Compared with the approximate BER under high SNR condition in Ref. [2], the presented analysis is more accurate for arbitrary SNR.
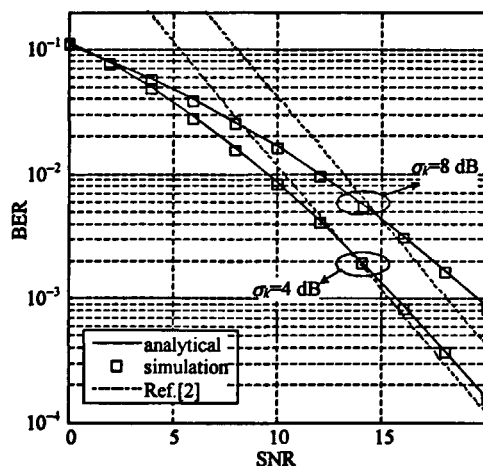

Fig. 2 BER performance of distributed Alamouti STBC with BPSK modulation versus SNR

4 Conclusions

This paper analyzed the BER performance for STBC with distributed transmit antennas, where Alamouti's scheme was employed. For BPSK modulation, an efficiently approximate expression of BER was derived. Comparison of analytical and simulation results validated the presented expression. For further work, we will generalize the BER analysis to higher order modulations such as the MPSK, MQAM or consider the scenario where there are some spatial correlations between two transmission channels.

参 考 文 献

[1] CASTANHEIRA D, GAMEIRO A. Distributed antenna system capacity scaling[J]. IEEE Wireless Communications, 2010, 17(3): 68-75.

[2] SHEN Y, TANG Y, KONG T, et al. Optimal antenna location for STBC-OFDM downlink with distributed transmit antennas in linear cells[J]. IEEE Communications Letters, 2007, 11(5): 387-389.

[3] HAN K Y, LEE S W, LIM J S, et al. Time-variant fading channel estimation by extended RLS[J]. IEICE Transactions on Communications, 2004, E87-B(6): 1715-1718.

[4] 张桦，朱近康. 基于隐式训练和加权最小二乘的迭代信道估计[J]. 华中科技大学学报(自然科学版), 2008, 36(4): 13-16.
ZHANG Hua, ZHU Jin-kang. Iterative channel estimation using superimposed training and weighted- least-square method[J]. Huazhong University of Science & Technilogy (Natural Science Edition), 2008, 36(4): 13-16.

[5] STOJANOVIC M. Retrofocusing techniques for high rate acoustic communications[J]. Journal of the Acoustical Society of America, 2005, 117(3): 1173-1185.

[6] DE BEEK V J J, EDFORS O, SANDELL M, et al. On channel estimation in OFDM systems[C]//The 1995 IEEE 45th Vehicular Technology Conference. Chicago: IEEE Press, 1995.

[7] KANG Y, KIM K, PARK H. Efficient DFT-based channel estimation for OFDM systems on multi-path channels[J]. IET Communications, 2007, 1(2): 197-202.

[8] 程历帮. OFDMA系统中基于LMMSE信道估计算法的改进及其性能分析[J]. 电子学报, 2008, 36(9): 1782-1785.
CHENG Lü-bang. An improved LMMSE channel estimation method and its performance analysis[J]. Acta Electronica Sinica, 2008, 36(9): 1782-1785.

[9] 郭业才. 自适应盲均衡技术[M]. 合肥: 合肥工业出版社, 2007.
GUO Ye-cai. Adaptive blind equalization technique[M]. Hefei: Hefei Industry Press, 2007.

[10] SAYED A H, KAILATH T. A state-space approach to adaptive RLS filtering[J]. IEEE Signal Processing Magazine, 1994, 11(3): 18-60.

编 辑 税 红

[3] ZHOU S, ZHOU M, XU X, et al. Distributed wireless communication systems: a new architecture for future public wireless access[J]. IEEE Communications Magazine, 2003, 41(3): 108-113.

[4] ALAMOUTI S M. A simple transmit diversity technique for wireless communications[J]. IEEE Journal on Select Areas in Communications, 1998, 16(8): 1451-1458.

[5] PAPADOPOULOS G D, KARAGIANNIDIS G K, PAVLIDOU F N. Performance bounds of space-time block coding in rician and log-normal fading channels[J]. IET Communications, 2007, 1(1): 86-91.

[6] CATREUX S, DRIESSEN P F, GREENSTEIN L J. Data throughputs using multiple-input multiple-output (MIMO) techniques in a noise-limited cellular environment[J]. IEEE Transactions on Wireless Communications, 2002, 1(2): 226-235.

[7] SIMON M K, ALOUINI M S. Digital communications over fading channels: a unified approach to performance analysis[M]. New York: Wiley, 2000.

[8] ANDREWS J G, GHOSH A, MUHAMED R. Fundamentals of WiMAX: Understanding broadband wireless networking[M]. Upper Saddle River, NJ: Prentice Hall, 2007.

[9] LEVER K V. New derivation of Craig's formula for the Gaussian probability function[J]. Electronics Letters, 1998, 34(19): 1821-1822.

[10] ABRAMOWITZ M, STEGUN I A. Handbook of mathematical function with formular, graphs, and mathematical tables[M]. New York: Dover Press, 1972.

编 辑 张 俊

如 何 学 习 天 线 设 计

　　天线设计理论晦涩高深，让许多工程师望而却步，然而实际工程或实际工作中在设计天线时却很少用到这些高深晦涩的理论。实际上，我们只需要懂得最基本的天线和射频基础知识，借助于 HFSS、CST 软件或者测试仪器就可以设计出工作性能良好的各类天线。

　　易迪拓培训(www.edatop.com)专注于微波射频和天线设计人才的培养，推出了一系列天线设计培训视频课程。我们的视频培训课程，化繁为简，直观易学，可以帮助您快速学习掌握天线设计的真谛，让天线设计不再难…

HFSS 天线设计培训课程套装

套装包含 6 门视频课程和 1 本图书，课程从基础讲起，内容由浅入深，理论介绍和实际操作讲解相结合，全面系统的讲解了 HFSS 天线设计的全过程。是国内最全面、最专业的 HFSS 天线设计课程，可以帮助你快速学习掌握如何使用 HFSS 软件进行天线设计，让天线设计不再难…

课程网址：http://www.edatop.com/peixun/hfss/122.html

CST 天线设计视频培训课程套装

套装包含 5 门视频培训课程，由经验丰富的专家授课，旨在帮助您从零开始，全面系统地学习掌握 CST 微波工作室的功能应用和使用 CST 微波工作室进行天线设计实际过程和具体操作。视频课程，边操作边讲解，直观易学；购买套装同时赠送 3 个月在线答疑，帮您解答学习中遇到的问题，让您学习无忧。

详情浏览：http://www.edatop.com/peixun/cst/127.html

13.56MHz NFC/RFID 线圈天线设计培训课程套装

套装包含 4 门视频培训课程，培训将 13.56MHz 线圈天线设计原理和仿真设计实践相结合，全面系统地讲解了 13.56MHz 线圈天线的工作原理、设计方法、设计考量以及使用 HFSS 和 CST 仿真分析线圈天线的具体操作，同时还介绍了 13.56MHz 线圈天线匹配电路的设计和调试。通过该套课程的学习，可以帮助您快速学习掌握 13.56MHz 线圈天线及其匹配电路的原理、设计和调试…

详情浏览：http://www.edatop.com/peixun/antenna/116.html

关于易迪拓培训：

易迪拓培训(www.edatop.com)由数名来自于研发第一线的资深工程师发起成立，一直致力和专注于微波、射频、天线设计研发人才的培养；后于 2006 年整合合并微波 EDA 网(www.mweda.com)，现已发展成为国内最大的微波射频和天线设计人才培养基地，成功推出多套微波射频以及天线设计经典培训课程和 ADS、HFSS 等专业软件使用培训课程，广受客户好评；并先后与人民邮电出版社、电子工业出版社合作出版了多本专业图书，帮助数万名工程师提升了专业技术能力。客户遍布中兴通讯、研通高频、埃威航电、国人通信等多家国内知名公司，以及台湾工业技术研究院、永业科技、全一电子等多家台湾地区企业。

我们的课程优势：

※ 成立于 2004 年，10 多年丰富的行业经验

※ 一直专注于微波射频和天线设计工程师的培养，更了解该行业对人才的要求

※ 视频课程、既能达到了现场培训的效果，又能免除您舟车劳顿的辛苦，学习工作两不误

※ 经验丰富的一线资深工程师主讲，结合实际工程案例，直观、实用、易学

联系我们：

※ 易迪拓培训官网：http://www.edatop.com

※ 微波 EDA 网：http://www.mweda.com

※ 官方淘宝店：http://shop36920890.taobao.com